ESAT-6-specific CD4 T cell responses to aerosol *Mycobacterium tuberculosis* infection are initiated in the mediastinal lymph nodes

William W. Reiley*, Mark D. Calayag[†], Susan T. Wittmer*, Jennifer L. Huntington[†], John E. Pearl*, Jeffrey J. Fountain*, Cynthia A. Martino*, Alan D. Roberts*, Andrea M. Cooper*, Gary M. Winslow*[†‡], and David L. Woodland*[‡]

*Trudeau Institute, 154 Algonquin Avenue, Saranac Lake, NY 12983; and [†]Wadsworth Center, New York State Department of Health, P.O. Box 22002, Albany, NY 12201-2002

CD4^{+} T cell responses to aerosol *Mycobacterium tuberculosis* (Mtb) infection are characterized by the relatively delayed appearance of effector T cells in the lungs. This delay in the adaptive response is likely critical in allowing the bacteria to establish persistent infection. Because of limitations associated with the detection of low frequencies of naïve T cells, it had not been possible to precisely determine when and where naïve antigen-specific T cells are first activated. We have addressed this problem by using early secreted antigenic target 6 (ESAT-6)-specific transgenic CD4 T cells to monitor early T cell activation *in vivo*. By using an adoptive transfer approach, we directly show that T cell priming to ESAT-6 occurs only after 10 days of infection, is initially restricted to the mediastinal lymph nodes, and does not involve other lymph nodes or the lungs. Primed CD4 T cells rapidly differentiated into proliferating effector cells and ultimately acquired the ability to produce IFN-γ and TNF-α *ex vivo*. Initiation of T cell priming was enhanced by two full days depending on the magnitude of the challenge inoculum, which suggests that antigen availability is a factor limiting the early CD4 T cell response. These data define a key period in the adaptive immune response to Mtb infection.

priming | transgenic mice

Tuberculosis is a major health problem in the world today (1). It is estimated that one-third of the world's population has been infected with *Mycobacterium tuberculosis* (Mtb), and although only 5–10% of infected individuals develop disease, ≈2 million deaths occur annually. The emergence of multidrug-resistant and extensively drug-resistant strains of Mtb threatens to overcome current control measures (2). Despite an urgent need to develop new vaccines and therapies, progress has been limited by a lack of basic understanding of how and where protective immune responses to Mtb are initiated and maintained.

Tuberculosis is predominantly a pulmonary disease acquired via aerosol infection. Protective immunity to Mtb infection depends upon CD4 T cells (3). Effector CD4 T cell responses have been detected in the mediastinal lymph node (MLN) and lung 2–3 weeks after low-dose infections, although studies by Chackerian *et al.* (4, 5) detected Mtb-specific IFN-γ-producing CD4 T cells as early as day 12 after infection in the lung-draining lymph node (LN). Similar detection techniques showed the T cell responses to other aerogenic infections, such as influenza, to be much more rapid (6), raising the question of why the response to Mtb is apparently delayed. Furthermore, the Mtb immune response has only been detected after Mtb has disseminated from the lungs (4, 7, 8). Because these studies of aerosol Mtb infection relied on the detection of effector T cells, it was not known whether priming had initially occurred in the lung or MLN or whether effector T cells had trafficked to these sites after Mtb dissemination. More recent studies of a population of Ag85-specific CD4 T cells demonstrated that T cell proliferation occurred first in the MLN, indicating that this tissue is a site of

T cell priming (5). These prior studies relied on indirect assessments of T cell priming (e.g., proliferation and cytokine production), however, and did not characterize the earliest events after antigen encounter. Delineation of these priming events will be important for understanding how protective immunity is generated against Mtb.

The reason for the delayed CD4 T cell response to Mtb is not completely understood. However, the apparent delay in the CD4 T cell response likely allows the bacteria sufficient time to establish persistent infection. One hypothesis to explain the lag in the adaptive immune response is that antigen is unavailable early after infection to initiate an immune response. For example, effector T cell responses were detected within 5 days after i.v. infection (9); these results were likely due to higher antigen loads. It is also unclear whether T cell priming can occur only after bacterial dissemination from the lungs to the draining LNs (4) or whether it requires that professional antigen-presenting cells (APCs) acquire antigen in infected lungs and migrate to secondary LNs (10). Another possible explanation for the delayed T cell response is that Mtb actively subverts antigen presentation (11).

The problem in analyzing the earliest events of T cell priming is that the frequency of naïve antigen-specific T cells is very low in uninfected mice. To overcome this problem, we have developed an Mtb-specific T cell receptor (TCR) transgenic mouse strain and have used T cells from these mice to experimentally increase the precursor frequency of antigen-specific T cells in infected mice (12). We show that CD4^{+} T cells specific for ESAT-6[1-20]/I-A[b] are primed in the MLN on day 10 after aerosol infection with 75 colony forming units (CFU) of Mtb. These data reveal that CD4 T cell responses during Mtb infection occur much later relative to many other respiratory infections. We also demonstrate that priming of naïve T cells during Mtb infection is limited by antigen and that priming is initially restricted to the MLN. These studies define directly a key early event in the development of protective immunity.

Results

Generation of an ESAT-6-Specific TCR Transgenic Mouse Strain. ESAT-6 is a relatively abundant secreted Mtb protein that is a major target of CD4^{+} and CD8^{+} T cells in both mice and humans
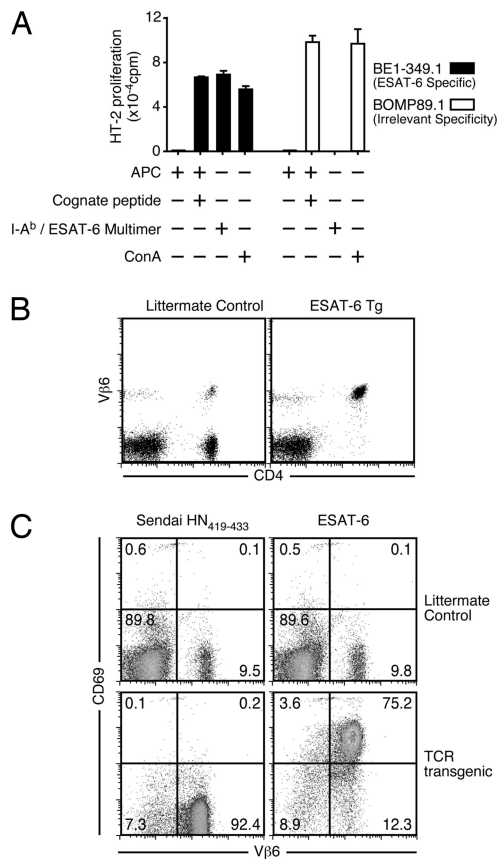
MICROBIOLOGY

Fig. 1. Generation of an ESAT-6_{1-20}/I-A^b-specific TCR transgenic mouse. (*A*) The ESAT-6_{1-20}/I-A^b-specific T cell hybridoma BE1-349.1 or the irrelevant hybridoma BOMP89.1 was stimulated with splenic APCs alone, APCs plus cognate peptide, an ESAT-6/I-A^b multimer (Trudeau Institute), or the mitogen concanavilan A (ConA), as indicated. IL-2 production was determined by measuring ^{3}H-thymidine incorporation by the IL-2-dependent cell line HT-2. (*B*) C57BL/6J littermates or C57BL/6J backcross progeny of transgenic founder mice were stained with antibodies against CD4 and Vβ6. The right dot plot is representative of the Vβ6 expression on CD4 T cells from a transgenic mouse. (*C*) Splenocytes from transgenic or littermate control mice were incubated for 24 h with spleen APCs plus Sendai HN$_{419-433}$ or ESAT-6_{1-20} peptides. The dot plots show up-regulation of CD69 expression on CD4-positive Vβ6-expressing transgenic T cells only after incubation with the specific peptide (upper right quadrant in bottom right plot).

during infection (13, 14). Our previous studies (8) demonstrated that CD4 T cells specific for ESAT-6 are a substantial population in lungs and lymphoid tissues of Mtb-infected mice after aerosol infection. These studies relied, however, on indirect measures of T cell effector functions. To facilitate the direct analysis of CD4 T cell responses, we generated a transgenic mouse strain that expresses TCR genes that encode a TCR specific for ESAT-6_{1-20} presented by the class II molecule I-A^b (15). The TCR genes were isolated from a T cell hybridoma (BE1-349.1) that recognizes ESAT-6_{1-20}/I-A^b (Fig. 1*A*). The hybridoma encodes a TCR containing the Vβ6 TCR chain, a commonly represented Vβ among IFN-γ-producing ESAT-6_{1-20}/I-A^b CD4 T cells during both the acute and chronic phases of Mtb infection (8, 14). Candidate TCRα and TCRβ genes were cloned in the human CD2 expression vector (16), and the construct was used to generate germ-line transgenic mice. F1 founder mice were identified based on their expression of Vβ6 on the majority of CD4 T cells (Fig. 1*B*). These F1 founder mice were back-crossed to C57BL/6J mice. To confirm the specificity of the T cells from the transgenic mice, we examined the ability of these cells to
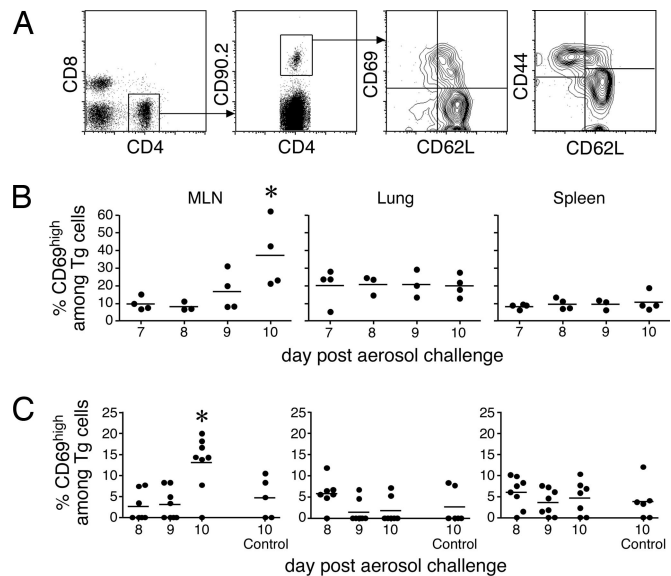

Fig. 2. Early activation occurred within 10 days after infection and was unaffected by donor T cell number. Naïve ESAT-6 transgenic cells (1 × 10^6) were isolated by negative magnetic bead selection and injected i.v. into Thy1.1-congenic recipient mice 1 day before aerosol infection with 75 CFU of Mtb (strain H37Rv). Four mice were analyzed each day from day 7 through day 10 after infection. (*A*) Diagram of the flow cytometric gating strategy used to analyze CD69 and CD44 expression by the activated transgenic T cells. (*B*) Expression of CD69 on donor ESAT-6 transgenic T cells in the spleen, MLN, and the lung on the indicated days after infection. The data are representative of two independent experiments. (*C*) B6.SJL-Ptrpca$^{+/-}$ (F1)-congenic hosts were injected with naïve ESAT-6 transgenic cells (5 × 10^4) on the day of aerosol infection. Expression of CD69 on donor ESAT-6 transgenic T cells in the MLN, spleen, and lung on the indicated days after infection is shown. (*B* and *C*) Data points are representative of individual mice. The horizontal bars indicate the mean of four to eight mice. The first days in which statistical significance was noted relative to control mice are indicated by asterisks. Statistical significance was determined by using the Student's *t* test ($P \leq 0.05$).

up-regulate CD69 *in vitro* when cultured with APC and ESAT-6_{1-20} peptide. Transgenic T cells were only activated in the presence of cognate peptide, demonstrating that the transgenic T cells exhibited the intended specificity (Fig. 1*C*).

Naïve T Cells Are First Activated on Day 10 in the MLN After Low-Dose Aerosol Mtb Infection. To analyze early events in the T cell response after Mtb infection, we used an adoptive transfer approach whereby 1 × 10^6 naïve ESAT-6_{1-20}/I-A^b-specific transgenic T cells were intravenously transferred into congenic-recipient Thy1.1 mice (12) 1 day before aerosol infection with 75 CFU of strain H37Rv (17). To directly identify the earliest encounter of the naïve T cell with antigen, we made use of the observation that naïve T cells rapidly up-regulate CD69 within the first few hours of antigenic contact (18). Specifically, we addressed when CD69 was first expressed on the donor transgenic T cells. Relatively high numbers of donor transgenic cells were used to facilitate the detection of early T cell priming. Approximately 20% of the transgenic T cells up-regulated CD69 on day 9 after infection in the MLN (Fig. 2*A* and *B*). To address concerns that the use of supraphysiological numbers of transgenic cells affected the results, the experiment was repeated using fewer transgenic cells. Similar activation kinetics were observed when 5 × 10^4 transgenic T cells were transferred on the same day as the aerosol inoculation, indicating that priming was independent of donor T cell numbers (Fig. 2*C*). Although 5 × 10^4 transgenic T cells were still supraphysiological, the use of

fewer donor T cells did not allow the recovery of sufficient numbers of donor cells to perform the analyses.

To eliminate a concern that factors secreted early during Mtb infection may suppress naïve T cell activation, we performed a second set of studies wherein we transferred 2×10^6 naïve ESAT-6/I-A^b-specific transgenic cells into recipient mice that had been infected 6 days earlier. In these studies, activation of the transgenic cells was assessed in secondary lymphoid and peripheral tissues by monitoring expression of the activation markers CD69, CD62L, and CD44. CD69 up-regulation was first observed on a portion of donor transgenic cells on day 10 after infection (Fig. 3 *A* and *B*). Activation occurred exclusively in the MLN, which drains the lower lung (Fig. 3 *A* and *B*), with no evidence of T cell priming in the lungs (Fig. 3*B*) or the cervical and mesenteric LNs [supporting information (SI) Fig. S1*A*]. Furthermore, the differentiation of newly activated cells (19) (identified by down-regulation of CD62L and up-regulation of CD44 surface expression) occurred 1–2 days after CD69 up-regulation and was initially restricted to the MLN (Fig. 3*B* and Fig. S1*A*). Within 14–15 days after infection, effector transgenic T cells were found in peripheral tissues, including the lung and spleen. The T cells in these tissues no longer expressed CD69. Because CD69 is rapidly down-regulated before LN emigration, the data suggest that the transgenic T cells in the lung and spleen were differentiated effector cells that were primed not locally, but rather in the MLN. Using the analyses described here, we were unable to detect activated endogenous T cells, likely because they were present at very low frequency (Fig. 3*C* and Fig. S1*B*).

In previous studies, effector T cell responses were detected only after Mtb emigration from the lung to the MLN (4). Because we observed priming in the MLN on day 10, we addressed whether viable bacteria were present in the MLN at this time after low-dose infection. Bacteria were detected in the MLNs of 4 of 12 mice assayed on day 9; by day 11, all mice contained viable bacteria in their MLNs (Fig. 3*D*). These data confirm the study by Chackerian *et al.* (4) and suggest that bacterial dissemination to the MLN and T cell priming are causally related.

Primed ESAT-6/I-A^b-Specific Transgenic T Cells Rapidly Acquire Effector Functions. We next investigated when and where the transgenic T cells acquired effector functions. The capacity of donor T cells to undergo cell division was examined by using a carboxyfluorescein diacetate succinimidyl ester (CFSE)-dilution assay (Fig. 4*A*). Cell division first occurred in the MLN on day 12 in most animals (Fig. 4*B* and Fig. S2*A*), and division was responsible for an increase in the number of transgenic T cells by day 14 in the MLN (Fig. 4*C* and Fig. S2*B*). We also addressed whether the transgenic CD4 T cells could produce inflammatory cytokines in response to specific antigen. Transgenic T cells isolated from the spleen, MLN, and lung of infected recipient mice produced IFN-γ and TNF-α in response to ESAT-6$_{1-20}$ as early as day 15 after infection (Fig. 4*D*). The majority of the T cells in the cultures produced cytokines *in vitro*, suggesting that most of the donor T cells had participated in the response *in vivo*. These data suggest that, by day 10, CD4 T cell responses are initiated in the MLN and are followed by cell proliferation, acquisition of effector functions, and migration to other anatomical locations.

The Kinetics of Naïve T Cell Priming Depends on the Challenge Inoculum During Mtb Infection. It is unclear why the initial CD4 T cell response to Mtb is delayed relative to other bacterial and viral infections. One possibility is that the late initiation of the Mtb-specific T cell response is a consequence of the slow replication of Mtb (the bacterium has a doubling time of 28 h), which limits the amount of available antigen. Although studies by North *et al.* (20)
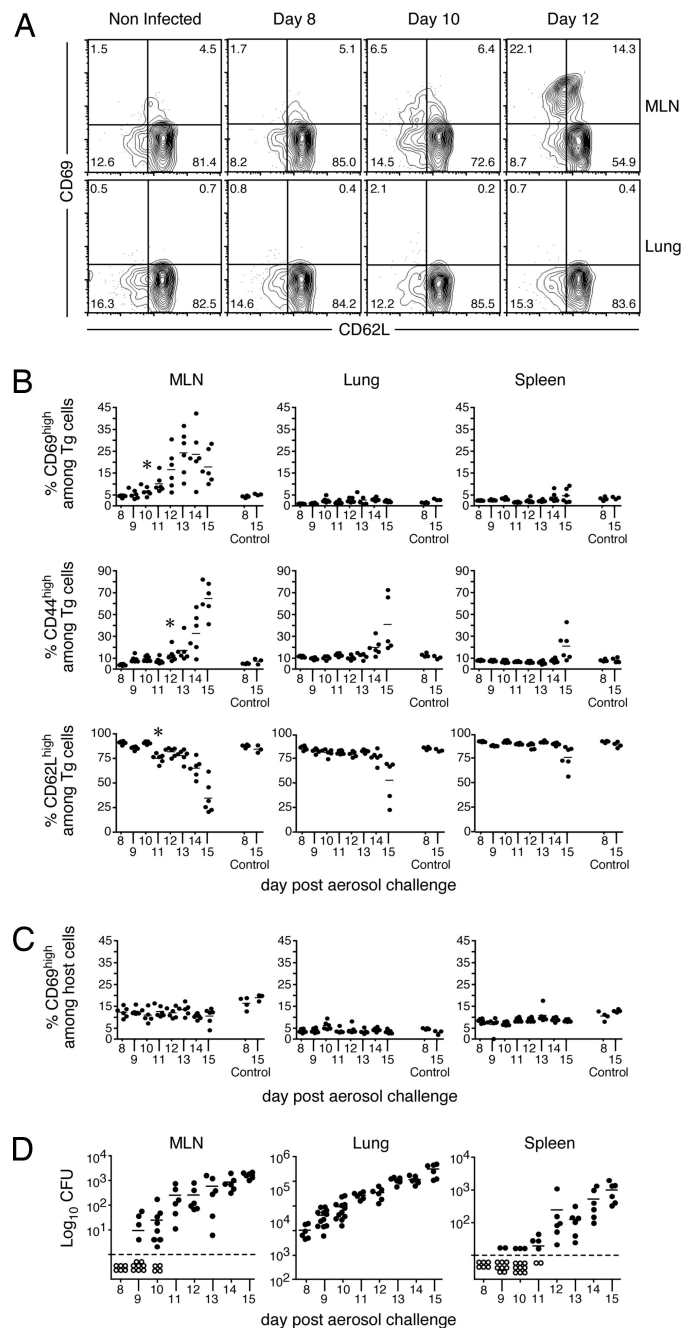

Fig. 3. Kinetics of ESAT-6/I-A^b-specific transgenic T cell activation during Mtb infection. Naïve ESAT-6 transgenic cells (2×10^6) were injected into Thy1.1-congenic hosts that had been aerosol-infected 6 days earlier with 75 CFU of Mtb. Six mice were analyzed each day from day 8 through day 15 after infection. Four noninfected control mice were included on days 8 and 15 after infection (Control 8 and 15, respectively). The data are representative of three independent experiments of similar design. (*A*) Representative dot plots of CD69 and CD62L expression on CD4$^+$/CD90.2$^+$ transgenic T cells isolated from MLNs and lungs of uninfected and Mtb-infected mice on days 8, 10, and 12 after infection. (*B*) Expression of CD69, CD44, and CD62L on donor ESAT-6 transgenic T cells in the MLN, lung, and spleen. (*C*) Expression of CD69 on endogenous (host) CD4 T cells within the same animals analyzed in *B*. (*D*) Dissemination of Mtb after aerosol infection. Mice were killed, and the Mtb CFUs in the indicated tissues was determined. The open symbols below the dashed line indicate that no viable bacteria were detected within the entire organ homogenate. Data points are representative of individual mice. The horizontal bars indicate the mean of four to six mice. The first days in which statistical significance was noted relative to control mice are indicated by asterisks.
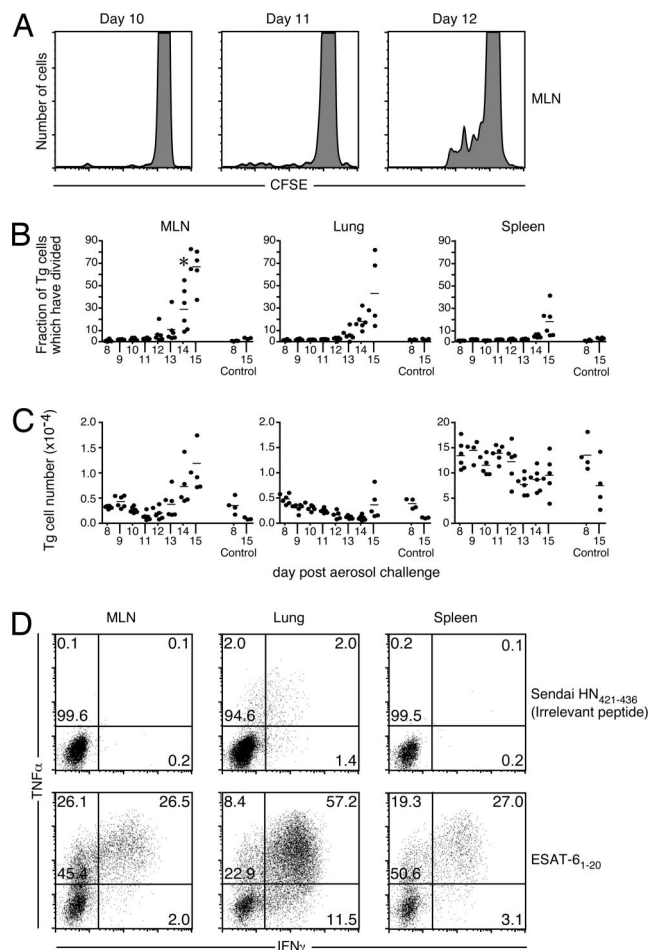
MICROBIOLOGY

Fig. 4. ESAT-6$_{1-20}$/I-A^b-specific transgenic T cells undergo differentiation and exhibit effector functions after Mtb infection. CFSE-labeled or unlabeled naïve ESAT-6 transgenic cells (2×10^6) were i.v. administered on day 6 to recipients that had been aerosol-infected with 75 ± 25 CFU of H37Rv. (*A*) A representative histogram of CFSE expression on CD4$^+$/CD90.2$^+$ transgenic T cells in the MLN on days 9–12 after infection. (*B*) The fraction of transgenic T cells that had undergone cell division were determined on the basis on CFSE dilution. Data are presented from the spleens, MLNs, and the lungs of six mice analyzed on each day from days 8–15 after infection. Four noninfected control mice were included on days 8 and 15 after infection (Control 8 and 15, respectively). The data are representative of two independent experiments of similar design. (*C*) The number of transgenic cells shown in *B* are indicated. (*D*) Mice that received unlabeled naïve ESAT-6 transgenic cells were analyzed on day 15 after infection for the production of IFN-γ and TNF-α. Cells isolated from each tissue were stimulated with either an irrelevant peptide (Sendai HN$_{421-436}$) or ESAT-6$_{1-20}$ for 6 h in the presence of brefeldin A. CD4$^+$/CD90.2$^+$ transgenic T cells are shown in the dot plots.

Fig. 5. The timing of naïve T cell activation and bacterial dissemination depends on the size of the Mtb inoculum. Naïve ESAT-6 transgenic cells (2×10^6) were i.v. injected into Thy1.1 congenic mice that had been aerosol-infected 5 days earlier with 75 ± 25, 600 ± 90, and $1,200 \pm 200$ CFU. (*A*) The expression of CD69 on donor ESAT-6$_{1-20}$/A^b transgenic T cells was analyzed in the MLN, lung, and spleen. (*B*) Expression of CD69 on host CD4 T cells in the high-inoculum-infected mice. The data are representative of two independent experiments of similar design and used three to six mice at each time point. Expression of CD69 on either host or transgenic CD4 T cells detected in individual Mtb-infected recipient mice is shown. (*C*) Mice were killed at the indicated times after infection, and the Mtb CFU in the indicated tissues was determined. The symbols indicate the CFU detected in each tissue after aerosol inoculation with 75 CFU (gray squares), 600 CFU (black circles), and 1200 CFU (white circles). Each datum represents a single mouse. Symbols below the horizontal dashed line indicate that viable bacteria were not detected within the entire organ homogenate. The asterisks are representative of statistical significance examined on each day between groups by using one-way ANOVA ($P \leq 0.05$). Statistically significant differences in lung bacterial burden between the groups were observed on each day after infection.

have shown that *esat6* (Rv3875) mRNA is detected *in vivo* within 10 days after infection, it is possible that ESAT-6 becomes available to T cells only after bacterial infection reaches a critical threshold. If bacterial burden and antigen availability are limiting factors, increasing the bacterial inoculum would be predicted to accelerate the kinetics of CD4 T cell priming. To test this hypothesis, mice were aerosol-infected with three doses of H37Rv (75 ± 25, 600 ± 90, and $1,200 \pm 200$ CFU), and naïve transgenic T cells were transferred to the infected mice on day 5 after infection. In mice that received the highest Mtb inoculum, naïve T cell activation was detected as early as day 8 after infection, 2 days earlier than was observed after our standard inoculum (Fig. 5). Having observed in Fig. 3*D* that dissemination is concomitant with T cell priming, we analyzed bacterial dissemination under these three challenge inoc-
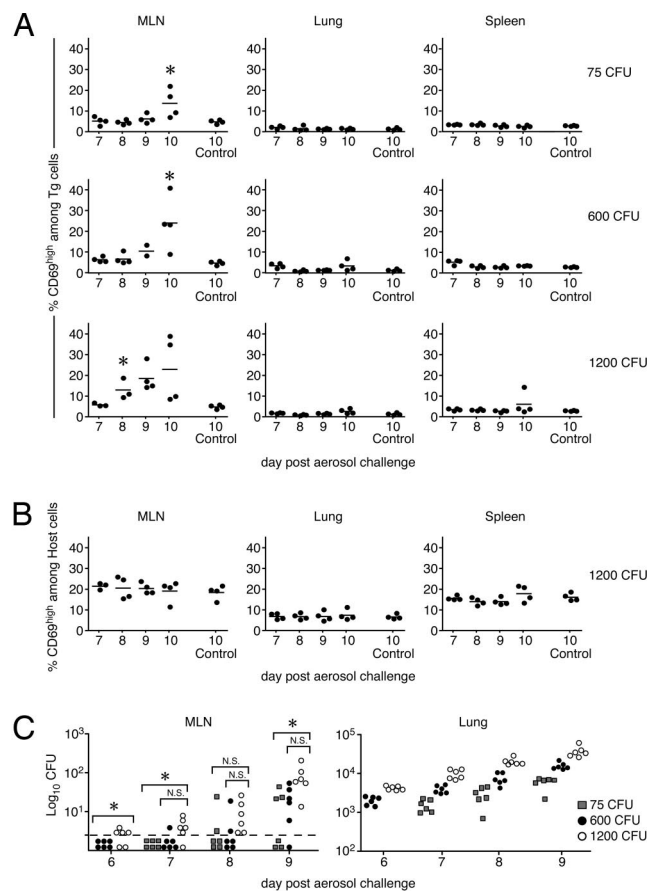
ulum conditions (Fig. 5*C*). Inoculum dose and bacterial dissemination were linked, demonstrating that T cell priming depends upon bacterial load and dissemination, which suggests that antigen availability is at least one factor influencing when T cell priming first occurs. Bacterial dissemination to the spleen was also enhanced by the higher inoculum doses on day 9 (data not shown).

Discussion

A key finding from our studies is that T cell responses to Mtb are initiated in the MLN $\approx$10 days after aerosol infection. This finding suggests that it takes at least 9 days for dendritic cells or other APCs to acquire antigen, mature, migrate to the LN, and initiate a T cell response (21). These kinetics are much delayed compared with those observed for acute viral infections (22, 23). Our conclusions are very similar to those from recently pub-

lished studies of the early activation of Mtb Ag85-specific CD4 T cells (5). In these related studies, activation was inferred to occur on day 11 based on proliferation data. The 1-day difference in activation kinetics may result from the use of an indirect vs. a direct measurement of T cell activation. Alternatively, the processing and presentation of the Ag85 peptide may be delayed relative to ESAT-6, or subtle differences in the experimental conditions may be responsible. Although our study and that by Wolf *et al.* (5) used supraphysiological numbers of naïve transgenic T cells in order to facilitate the detection of the early responding T cells, we demonstrated that our findings were not affected by the number of naïve T cells transferred or the timing of transfer relative to infection, because the transfer of as few as 5×10^4 transgenic cells on the day of infection yielded data equivalent to that obtained using larger numbers of donor cells on day 6 after infection. Although it is well known that naïve T cell frequency is an important factor in the generation of fully functional effector and memory T cells (24), our use of supraphysiological numbers of T cells allowed us to precisely determine when and where ESAT-6 was presented to CD4 T cells within Mtb-infected animals.

Although the CD4 T cell response to ESAT-6 does not appear to be initiated until day 10 after infection, the response progresses rapidly thereafter. Indeed, after the initial activation event (measured by CD69 up-regulation), the rate at which cells acquire an activated phenotype and begin to proliferate during Mtb infection is similar to that observed in other studies that have used CD4 T cell transgenic mouse models to study infections (for examples, see refs. 22 and 23). These data reveal that there is no difference in the kinetics of effector CD4 T cell responses between Mtb and other viral and bacterial systems. Once T cell activation is initiated, Mtb does not inhibit CD4 T cell responses during acute infection. Thus, the apparent delay in the appearance of effector cells during Mtb infection is due to a lack of sufficient antigen presentation before day 10 after infection rather than a delay in effector T cell differentiation.

It is unclear whether the relatively late initiation of the adaptive immune response is due to insufficient numbers of APCs or limited availability of antigen. One possibility is that slow bacterial growth and/or tissue sequestration results in a delay in antigen presentation (10). Because priming depends on the challenge inoculum, our data suggest that antigen is limiting. An alternative possibility is that antigen simply fails to trigger naïve T cells, perhaps because of bacterial subversion. In this regard, the 19-kDa lipoprotein from Mtb, which has been shown to inhibit class II expression in macrophages, could potentially interfere with naïve T cell priming (11).

Our work demonstrates that after low-dose aerosol infection naïve T cells become primed in the MLN but not in the lung. Although some other studies have suggested that T cell priming can be initiated in the lung itself (perhaps through the development of local lymphoid structures) (25), our data are consistent with reports that early T cell priming occurs only in the MLN (5). The role of dendritic cells in this process is unresolved. The dissemination of viable bacteria to the spleen before the appearance of activated transgenic cells (CD62L^{lo}/CD44^{hi}) and/or activation of naïve transgenic cells (CD62L^{hi}/CD44^{lo}) indicates that dissemination and antigen presentation are not always concurrent (Fig. 3*D*) (4). Although this study has addressed initial priming events, which are restricted to the MLN, we have yet to resolve whether bacterial dissemination is required to prime naïve T cells in secondary lymphoid organs, such as the spleen.

Taken together, our data identify the early events of a T cell response to an important early secreted protein using a low-dose aerosol Mtb infection. The development of successful vaccination strategies will be facilitated by a better understanding of how both CD4 and CD8 T cell responses are generated and sustained during an Mtb infection.

Methods

Generation of the Transgenic Mice. The CD4 T cell hybridoma BE349.1 was generated and cloned by using standard methods after s.c. immunization of C57BL/6 mice with ESAT-6$_{1-20}$ peptide emulsified in complete Freund's adjuvant (26). A panel of Vβ-specific antibodies were used to identify the TCR β-chain used (Vβ 6). To identify TCR transcripts expressed by the hybridomas, cDNA was screened by PCR by using a panel of oligonucleotides designed to identify each of the Vβ and Vα chain mRNAs (Table S1; provided by John Kappler, National Jewish Medical and Research Center, Denver). Amplicons were cloned into the TA Cloning Vector (Invitrogen), and the nucleotide sequences were determined to confirm that the Vα genes were intact. The cloned regions containing each of the genes were excised by using 5′ and 3′ EcoRI sites within the cloning vector and were inserted separately into the expression vector phCD2 (27) that had been restricted by using EcoRI.

To verify that the expressed genes encoded a TCR of the intended specificity, the expression plasmids were restricted with NotI and were introduced into the TCR loss-variant hybridoma 5KC.53.6.1 (28). After identification of transfectants that responded to I-A^b/ESAT6$_{1-20}$, the entire mouse coding and noncoding regions were excised from the hCD2 expression plasmid by using KpnI and NotI and were used for microinjection of mouse embryos (performed at the Van Andel Institute, Grand Rapids, MI).

Animals. C57BL/6J and B6.PL-Thy1a/Cy (Thy1.1) mice were purchased from The Jackson Laboratory. B6.SJL-Ptrpca$^{+/-}$ (F1) mice were generated and maintained in specific pathogen-free facilities at Trudeau Institute. ESAT-6 transgenic mice were generated as described above at the Van Andel Institute and subsequently back-crossed onto C57BL/6J. ESAT-6 transgenic mice were screened for expression of Vβ6 on CD4$^+$ T cells from the peripheral blood. Experimental mice were age- and sex-matched and used between 8 and 12 weeks. Mice were used in accordance with the Institutional Animal Care and Use Committee guidelines of the National Research Council and the Trudeau Institute.

Infections. The H37Rv stain of Mtb was grown in Proskauer Beck medium containing 0.05% Tween 80 to mid-log phase and frozen in 1-ml aliquots at $-70°C$. For aerosol infections, subject animals were infected with a low dose ($\approx$75 CFU) unless otherwise stated by using a Glas-Col airborne infection system as described (17). Bacterial burden was measured either through serial dilutions or with whole organ homogenate as described (17). CFUs from serial dilutions were determined based on total volume of tissue homogenate.

Lymphocyte Isolation and Flow Cytometry. Lung tissue was prepared by injecting tissue with a 0.5 mg/ml solution of Collagenase (Roche); the tissue was coarsely chopped and was incubated for 30–45 min at 37°C. Single-cell suspensions were prepared from lung tissue, LNs, or spleens by dispersing the tissues through a 70-μm nylon tissue strainer (Falcon). Single-cell suspensions were treated with Gey's solution to remove any residual red blood cells. Lymphocytes were enriched from lung tissue by isolation by using an 80/40% Percoll gradient. Single-cell suspensions were stained with fluorochrome-labeled antibodies for anti-CD4 (clone RM4-5), anti-CD8 (clone 5H10), and anti-CD62L (clone MEL-14) from Caltag; anti-CD90.2 (53-2.1) and anti-CD69 (H1.2F3) from BD Biosciences; and anti-CD44 (IM7) from eBioscience. The samples were analyzed on a CyAn ADP flow cytometer (DakoCytomation). The data were analyzed with FlowJo software (Tree Star).

CFSE-Labeling and Adoptive Transfer. Naïve transgenic CD4$^+$ T cells were isolated from various lymphoid tissues from transgenic mice. Single-cell suspensions were prepared as described above and were panned on goat anti-mouse IgG H+L (Jackson ImmunoResearch)-coated Primaria flasks (Falcon) for 30–45 min at 37°C to remove B cells and macrophages. The transgenic cells were next enriched by using a CD4$^+$ T cell negative isolation kit (Miltenyi Biotech). A sample of the sorted cells was analyzed to confirm purity and to evaluate the expression of the activation markers CD69, CD62L, and CD44. In some studies, transgenic T cells were labeled with 0.5 μM CFSE for 10 min at 37°C. Transgenic T cells (200 μl) were transferred i.v. into congenic mice on day 6 after infection with Mtb unless otherwise stated.

Intracellular Cytokine Detection. Lymphocytes isolated from infected mice as described above were incubated in a 96-well plate at a concentration of 3×10^6 cells. Cells were incubated in the presence of ESAT-6$_{1-20}$ or Sendai HN$_{421-436}$ peptide (5 μg/ml each) for 2 h at 37°C; Brefeldin A (50 μg/ml) was added, and the incubation was continued for an additional 4 h. Surface staining for CD4, CD8, and CD90.2 was performed as described previously (8), and the cells were fixed in 2% formaldehyde in PBS overnight. For detection of intracellular IFN-γ and TNF-α, the cells were incubated for 30 min in PBS containing 0.5% saponin

MICROBIOLOGY

(Sigma–Aldrich) followed by incubation in the same buffer with anti-IFN-γ (clone XMG1.2) and anti-TNF-α (clone MP6-XT22) for 30 min; the cells were then washed and analyzed as described above.

Statistical Analysis. Differences between the means of experimental groups were analyzed by using Student's *t* test (Prism 4 software, GraphPad). Differences were considered significant when $P \leq 0.05$.

1. Maartens G, Wilkinson RJ (2007) Tuberculosis. *Lancet* 370:2030–2043.
2. Raviglione MC, Smith IM (2007) XDR tuberculosis—Implications for global public health. *N Engl J Med* 356:656–659.
3. North RJ, Jung YJ (2004) Immunity to tuberculosis. *Annu Rev Immunol* 22:599–623.
4. Chackerian AA, Alt JM, Perera TV, Dascher CC, Behar SM (2002) Dissemination of *Mycobacterium tuberculosis* is influenced by host factors and precedes the initiation of T-cell immunity. *Infect Immun* 70:4501–4509.
5. Wolf AJ, et al. (2008) Initiation of the adaptive immune response to *Mycobacterium tuberculosis* depends on antigen production in the local lymph node, not the lungs. *J Exp Med* 205:105–115.
6. Flynn KJ, et al. (1998) Virus-specific CD8$^+$ T cells in primary and secondary influenza pneumonia. *Immunity* 8:683–691.
7. Lazarevic V, Myers AJ, Scanga CA, Flynn JL (2003) CD40, but not CD40L, is required for the optimal priming of T cells and control of aerosol *M. tuberculosis* infection. *Immunity* 19:823–835.
8. Winslow GM, Roberts AD, Blackman MA, Woodland DL (2003) Persistence and turnover of antigen-specific CD4 T cells during chronic tuberculosis infection in the mouse. *J Immunol* 170:2046–2052.
9. Cooper AM, Callahan JE, Keen M, Belisle JT, Orme IM (1997) Expression of memory immunity in the lung following re-exposure to *Mycobacterium tuberculosis. Tuber Lung Dis* 78:67–73.
10. Khader SA, et al. (2006) Interleukin 12p40 is required for dendritic cell migration and T cell priming after *Mycobacterium tuberculosis* infection. *J Exp Med* 203:1805–1815.
11. Pennini ME, Pai RK, Schultz DC, Boom WH, Harding CV (2006) *Mycobacterium tuberculosis* 19-kDa lipoprotein inhibits IFN-gamma-induced chromatin remodeling of MHC2TA by TLR2 and MAPK signaling. *J Immunol* 176:4323–4330.
12. Kearney ER, Pape KA, Loh DY, Jenkins MK (1994) Visualization of peptide-specific T cell immunity and peripheral tolerance induction *in vivo. Immunity* 1:327–339.
13. Ulrichs T, Anding P, Porcelli S, Kaufmann SH, Munk ME (2000) Increased numbers of ESAT-6- and purified protein derivative-specific gamma interferon-producing cells in subclinical and active tuberculosis infection. *Infect Immun* 68:6073–6076.
14. Sorensen AL, Nagai S, Houen G, Andersen P, Andersen AB (1995) Purification and characterization of a low-molecular-mass T-cell antigen secreted by *Mycobacterium tuberculosis. Infect Immun* 63:1710–1717.
15. Brandt L, Oettinger T, Holm A, Andersen AB, Andersen P (1996) Key epitopes on the ESAT-6 antigen recognized in mice during the recall of protective immunity to *Mycobacterium tuberculosis. J Immunol* 157:3527–3533.
16. Kouskoff V, Signorelli K, Benoist C, Mathis D (1995) Cassette vectors directing expression of T cell receptor genes in transgenic mice. *J Immunol Methods* 180:273–280.
17. Roberts AD, et al. (2002) Murine models of tuberculosis. *Methods in Microbiology*, eds Kaufmann S, Kabelitz D (Academic, London), pp 433–462.
18. Testi R, Phillips JH, Lanier LL (1989) Leu 23 induction as an early marker of functional CD3/T cell antigen receptor triggering. Requirement for receptor cross-linking, prolonged elevation of intracellular [Ca++] and stimulation of protein kinase C. *J Immunol* 142:1854–1860.
19. Stockinger B, Bourgeois C, Kassiotis G (2006) CD4+ memory T cells: Functional differentiation and homeostasis. *Immunol Rev* 211:39–48.
20. Rogerson BJ, et al. (2006) Expression levels of *Mycobacterium tuberculosis* antigen-encoding genes versus production levels of antigen-specific T cells during stationary level lung infection in mice. *Immunology* 118:195–201.
21. McSorley SJ, Asch S, Costalonga M, Reinhardt RL, Jenkins MK (2002) Tracking salmonella-specific CD4 T cells *in vivo* reveals a local mucosal response to a disseminated infection. *Immunity* 16:365–377.
22. Lawrence CW, Braciale TJ (2004) Activation, differentiation, and migration of naive virus-specific CD8+ T cells during pulmonary influenza virus infection. *J Immunol* 173:1209–1218.
23. Roman E, et al. (2002) CD4 effector T cell subsets in the response to influenza: Heterogeneity, migration, and function. *J Exp Med* 196:957–968.
24. Blair DA, Lefrancois L (2007) Increased competition for antigen during priming negatively impacts the generation of memory CD4 T cells. *Proc Natl Acad Sci USA* 104:15045–15050.
25. Moyron-Quiroz JE, et al. (2004) Role of inducible bronchus associated lymphoid tissue (iBALT) in respiratory immunity. *Nat Med* 10:927–934.
26. Woodland DL, et al. (1993) Major histocompatibility complex-specific recognition of Mls-1 is mediated by multiple elements of the T cell receptor. *J Exp Med* 177:433–442.
27. Zhumabekov T, Corbella P, Tolaini M, Kioussis D (1995) Improved version of a human CD2 minigene based vector for T cell-specific expression in transgenic mice. *J Immunol Methods* 185:133–140.
28. Huseby ES, et al. (2005) How the T cell repertoire becomes peptide and MHC specific. *Cell* 122:247–260.